Cluster observations of plasma sheet activity during the September 14-28, 2003 corotating high speed stream event

A. Korth, E. Echer, F. L. Guarnieri, M. Fränz, R. Friedel, W. D. Gonzalez, C. G. Mouikis, and H. Rème

Abstract:
In recent years there has been renewed discussion on the nature of recurrent substorm activity in the magnetosphere and their causative drivers. There is an active debate on periodic substorm versus sawtooth events, and triggered versus non-triggered substorms. We perform here a cross-wavelet analysis between the solar wind drivers and the plasmasheet at $\sim$ 20 R_E and geosynchronous responses during the September 2003 high speed stream event, using ACE, Cluster and LANL geosynchronous data. We show that the magnetospheric response with a periodicity of 2-4 hours is well correlated with the Alfvén wave structure embedded in the fast streams. This indicates that the recurrent activity observed here is directly driven in contrast to the periodic sawtooth events which occur under conditions of steady driving.

Key words: substorms, plasma sheet, geosynchronous orbit.

1. Introduction

The question of what external or internal events cause or trigger recurring periodic substorms has been one of the fundamental issues of substorm research, and one on which there is as yet no consensus.

Individual substorm occurrence has been linked to northward turnings of the interplanetary magnetic field (IMF) at the end of intervals of southward IMF [10, 3]. While random or isolated substorms form the largest class of events, periodic substorms are often observed with inter-substorm times of around 3 hours [4].

Periodic activity, such as during sawtooth events, has been directly correlated with corresponding solar wind dynamic pressure enhancements [9]. Others suggest that sawtooth events can be viewed as a magnetospheric mode similar to Steady Magnetospheric Convection intervals (SMCs) except that for sawtooth events, the flow of energy from the solar wind into the magnetosphere becomes too large to dissipate without the periodic occurrence of substorms. They further suggest that the quasi-periodicity arises because the magnetosphere may only become susceptible to external or internal triggering after it has been driven beyond a stability threshold. This can account for the existence of more potential external triggers (in the interplanetary magnetic field or solar wind) than teeth, namely that the magnetosphere may be selectively responsive to such a structure [7].

During the descending and minimum phases of solar cycles, CMEs become less frequent and another type of solar structure occur more often: coronal holes. Coronal holes are open magnetic field regions, from where high speed solar wind streams emanate [15, 16, 17, 6]. High speed streams have velocities much higher than the typical velocities observed in the solar wind, forming an interface region between the slow and fast streams. At large heliocentric distances (typically larger than 1 AU), these stream interface/interaction regions are bounded by a pair of shocks [18].

Since coronal holes are long lived structures, they can persist for more than one solar rotation, and the high speed streams originated from the same region reappear at intervals of approximately 27 days [18]. This reappearance leads to the term "recurrent stream". The spiral-like structure formed by these streams, distorted due to the solar rotation, and its interaction regions with slower streams, is known as Corotating Interaction Region (CIR).

For this study, an important aspect of these fast streams is that they are embedded with Alfvén waves [2]. These Alfvén waves are believed to be remnants of heating processes in the solar corona [8]. In the interplanetary data, these waves appear as large amplitude oscillations in magnetic field components with periods from a few minutes to a few hours, well correlated with the oscillations of the velocity components in the same direction [2, 21].

When these structures reach the Earth, they can lead to the development of a geomagnetic storm, due to the compressed plasma region in front of the high speed stream, the increase in the velocity, and the presence of Alfvén waves. Relativistic electron energization and flux enhancements occur in association with high-speed solar wind streams and the Alfvén waves embedded in them [11]. These Alfvén waves, with intermittent negative IMF B_z and large IMF y-component $|B_y|$, may lead to significantly enhanced magnetospheric convection and thus substorm activity. We intend to show in this paper that the periodic substorm activity observed during the September 2003 high speed stream event is directly correlated with the

Received 2 June 2005.

A. Korth and M. Fränz. MPI für Sonnensystemforschung, Katlenburg-Lindau, Germany.
E. Echer, F. L. Guarnieri, and W. D. Gonzalez. INPE, Sao Jose dos Campos, Brazil
R. Friedel. LANL, Los Alamos, NM, USA
C. G. Mouikis. UNH, Durham, NH, USA
H. Rème. CESR, Toulouse, France

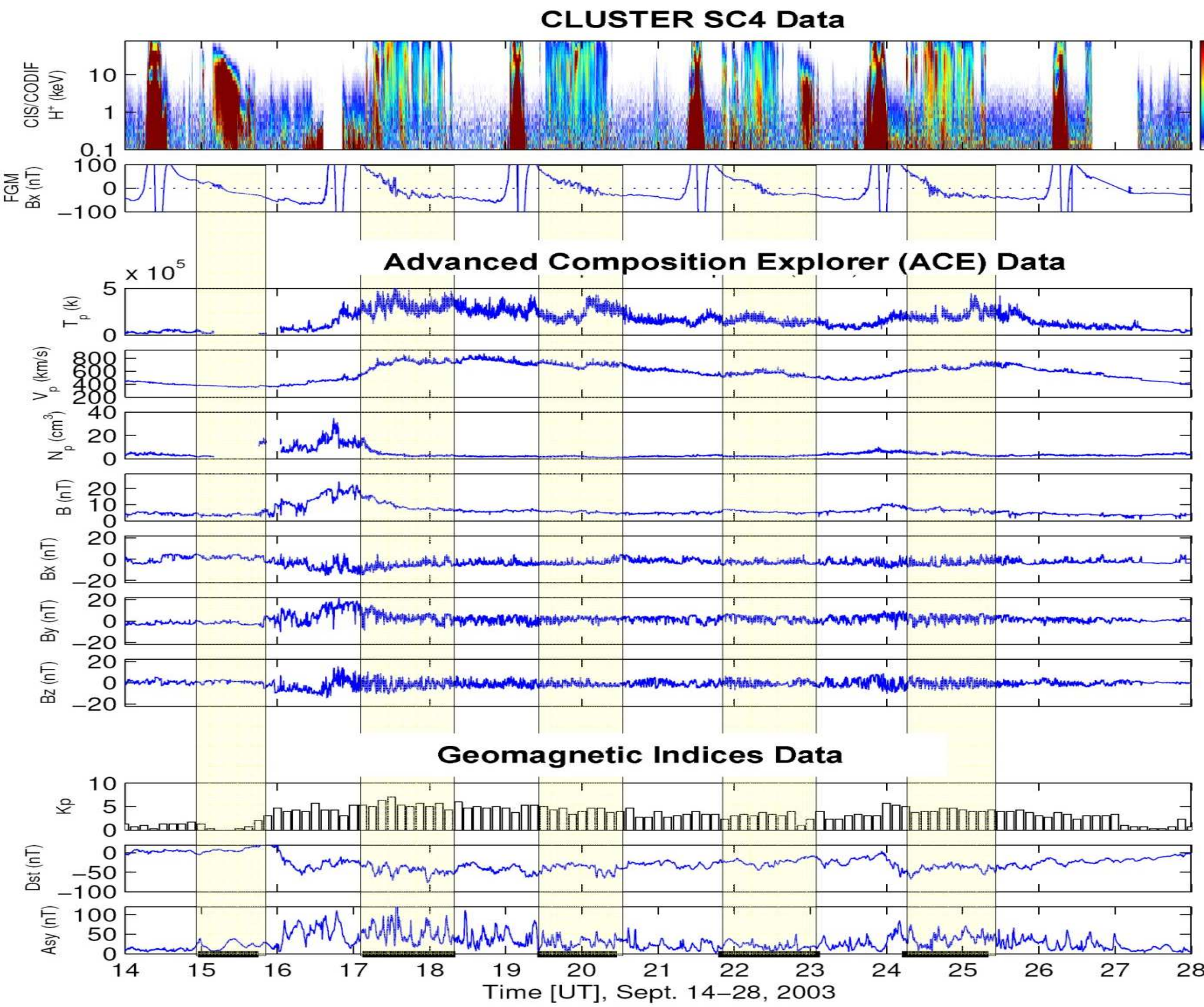

Fig. 1. Overview of the plasma sheet, the solar wind, and geomagnetic conditions for the September 14-28, 2003 period.

Alfvén wave periodicity observed in the solar wind.

2. Observations

This study uses particle and magnetic field measurements from Cluster SC4 [5], velocity, density and magnetic field measurements from the Advanced Composition Explorer (ACE) [19], and Los Alamos geosynchronous orbit data [14] during the September 14-28, 2003 corotating high speed stream event. The four Cluster satellites are in highly elliptical orbits, with apogee at 19.8 R_E and perigee of 4.0 R_E. In the September period the Cluster tetrahedron shows small distances of 2000 km between the satellites, so that only data from one spacecraft are used in the magnetospheric plasma sheet. The four Cluster spacecraft crossed the tail from north to south in the midnight sector between 23:00 and 24:00 LT.

We use particle data from the Cluster Ion Spectrometry (CIS) plasma instrument [13], the Cluster energetic particle spectrometer RAPID (Research with Adaptive Particle Imaging Detectors) [22], and the Flux Gate Magnetometer FGM [1]. The CIS data shown in this paper are from the COmposition and DIstribution Function (CODIF) analyzer, which is one of the sensors of the CIS instrument. CODIF measures the 3-dimensional distribution functions of the major ion species in the energy per charge range 0.03-40 keV/e. The RAPID spectrometer performs species identification with a time-of-flight measurement in the energy range from 50 to 1500 keV for protons and 30 to 300 keV for electrons.

3. Results

In Figure 1 we present an overview of the magnetotail plasma sheet, solar wind, and geomagnetic conditions for the September 14-28 period. In the first two panels the CIS/CODIF H^+ energy spectrogram and the B_x-component of the magnetic field in GSE coordinates are shown for Cluster SC4. The yellow high-lighted areas indicate time periods when Cluster SC4 crosses the plasma sheet in the magnetotail. Thick black horizontal bars are given in addition on the time axis for these crossings. The positive B_x-component of the magnetic field is directed towards the Sun and the negative towards the tail of the magnetosphere. Therefore it is an excellent indicator to show the magnetic equatorial crossings near perigee (large field) and apogee (small field). The proton spectrogram in the first panel shows during the first tail traversal (first high-lighted time interval) a cold plasma sheet. The plasma sheet is hotter after the arrival of the fast solar wind in the second and third highlighted period.

In the next panels solar wind plasma parameters and the interplanetary magnetic field are shown from the ACE spacecraft. In particular the density (N_p), the velocity (V_p), and the total magnetic field (B_t) with its components in GSE coordinates are given. The bottom panels show the Kp, Sym, and Asy geomagnetic activity indices. The Sym index is a 1-min version of the D_{st} index, and the Asy index indicates the level of asymmetries in the ring current.

The solar wind behavior was dominated by the presence of a large coronal hole which was just left of central meridian in the beginning of the period. The signature of the interaction region and the high speed stream is observed from September 15, 2003 to September 28, 2003. The first signs of it were noted as a slight increase in the solar wind velocity (from 355 to 380 km·s^{-1}) and a large density enhancement in the solar wind recorded by ACE on Sept 15, between 18:20 UT and midnight due to the compression of the solar wind in front of the high speed stream. Later a slow but steady increase of the solar wind speed was noted peaking at 800 km·s^{-1} around noon on September 18. The interplanetary magnetic field B_z was mostly southward-directed during the beginning of the event with its minimum at -15 nT on September 16 in the afternoon. Later from September 17, large amplitude Alfvén waves were observed in all three magnetic field components with amplitudes of plus/minus 10 nT especially in the B_z-component, which is responsive not to reconnection on the front side of the Earth and the energy input into the magnetosphere. The Alfvén waves continued during the passage of the interaction region until September 27, 2003.

The average speed and density of the slow solar wind, measured in the first yellow highlighted area were approximately 365 km·s^{-1} and 2.3 protons·cm^{-3}. The He^{++}/H^{+} ratio (not shown in the figure) was $\sim$ 0.1 and the total magnetic field was approximately 4 nT. In the interaction region the observed densities were 30 protons·cm^{-3} and the total magnetic field 20 nT. In the second yellow highlighted period - the beginning of the first high speed stream - the average solar wind was approximately 720 km·s^{-1} and the density was 4 protons·cm^{-3}. A sharp decrease in the density to 2 protons·cm^{-3} were observed. The average total magnetic field showed the same behavior as the density, with a sharp decrease to approximately 5 nT. In the next two yellow highlighted periods (3 and 4) a decrease in the solar wind speed and density is seen and the magnetic field remained on the same level of $\sim$ 5 nT. In the last highlighted period the solar wind speed, the density, and the total magnetic field increased again resulting from the interaction of a second high speed stream with the first one. During this period an increase in the He^{++} abundance was observed.

The geomagnetic field was initially at quiet levels ($K_p < 3$) but switched to a major storm regime on September 16 and even severe storm regime (K_p = 7) on September 17. The geomagnetic conditions persisted until September 27. During the first yellow highlighted period the average K_p index was approximately 1-, the average D_{st} index was slightly positive (6.7 nT) and the average Asy index was $\sim$ 21 nT. The D_{st} and the Asy index reached their peak values of -50 nT and +100 nT, respectively, during the passage of the interaction region, indicating the occurrence of a moderate magnetic storm. During the passage of the high speed stream the geomagnetic indices indicated a constant level of activity, decreasing during the 4th highlighted period and increasing again in the 5th highlighted period, when a second interaction region arrived.

Figure 2 shows the Cluster plasma sheet crossing during disturbed conditions on September 17 and 18, 2003, the second highlighted period at the beginning of the first high speed stream. From top to bottom we plotted an electron spectrogram in the energy range from 30-300 keV, and a proton spectrogram in the energy range from 50 to 1500 keV from the Cluster SC4 RAPID instrument, and a CIS proton spectrogram with its pitch angle distribution in the energy range from 0.03 to 40 keV/e. Further we present magnetic field data from Cluster in GSE coordinates, the theta angle (angle between the z-axis and the xy-plane, +z-axis north), the total (magnetic plus kinetic) pressure in nPa, and the plasma Beta parameter. The B_x-component of the magnetic field indicates where Cluster SC4 crosses the magnetic equator. The theta angle points out how much the magnetic field is stretched. β = 1 implies that the spacecraft is in the plasma sheet, and β = $<$ 1 means that it is in the plasma sheet boundary layer or even in the lobes.

We observe a hot and disturbed plasma sheet. The spacecraft during its traversal moves in and out of the plasma sheet. In the time intervals A, C, and E the spacecraft is inside the plasma sheet and in the intervals B and D outside of the plasma sheet in the lobes. Inside the plasma sheet we observe electrons up to 300 keV and protons up to 1000 keV. The spacecraft crosses the magnetic equator three times between 11:00 and 14:00 UT (B_x = 0). Due to an intermittently large negative IMF B_z there is a continuous energy input into the magnetosphere and into the magnetotail. This can be observed in the total pressure (kinetic and magnetic) which increases and decreases three times on September 17, 2003 in the time interval from 14:00 to 24:00 UT. During the pressure increase, the magnetic field stretches, and during the decrease the field dipolarizes which can also be observed in the theta angle of B in panel 6. These pressure changes are comparable to a loading and unloading process also called the growth and recovery phase of a substorm. During the growth phase, the total pressure increases from 0.2 to 1 nPa, the tail magnetic field stretches and the spacecraft moves out of the plasma sheet into the tail lobe. In the lobe the total pressure is similar to the magnetic pressure while the kinetic pressure is almost zero. At the end of the growth phase the tail field dipolarizes or thickens and the spacecraft is back in the plasma sheet.

During quiet solar wind conditions on September 14 and 15, 2003 (not shown) we find a cold plasma sheet with an energy of less than 40 keV and an isotropic H^{+} pitch angle distribution. We find a few counts in the electron and proton energy channels at higher energies above 30 keV. The total pressure is very low at 0.2 nPa.

In order to investigate the coupling power from the solar wind into the magnetotail, we have calculated the cross-wavelet power between ACE B_z and Cluster B_x data. We used the Mor-

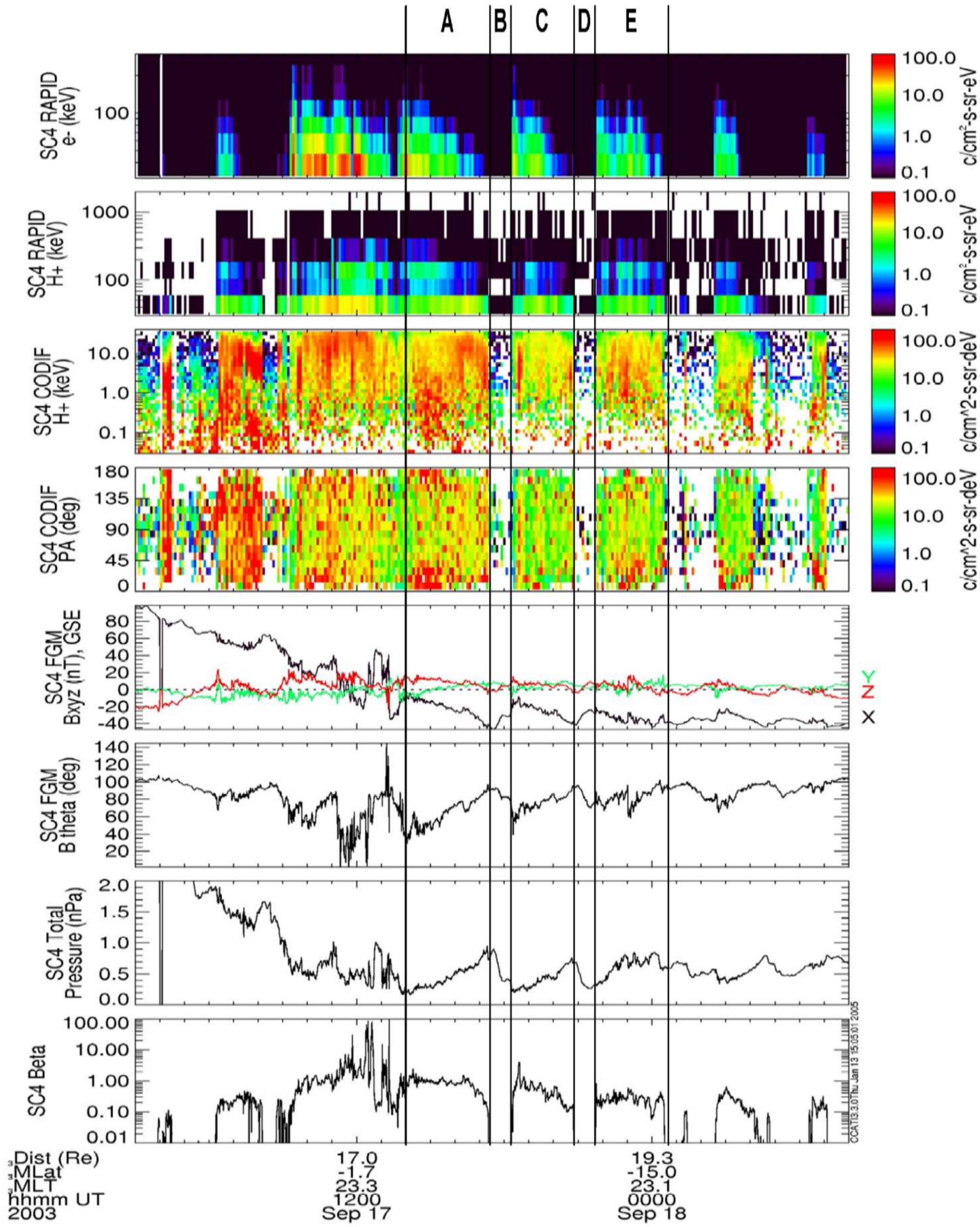

Fig. 2. Cluster plasma sheet crossing during a high speed stream and large IMF B_z amplitudes of more than $\pm$ 10 nT on September 17 and 18, 2003. From top to bottom: energy spectrograms of electrons and protons from RAPID, energy and pitch angle spectrograms of protons from CIS, x-,y-,z-components and theta from FGM, total (kinetic and magnetic) pressure, and beta.

let wavelet analysis [20, 12], because it is the most adequate to detect variations in the periodicities of geophysical signals in a continuous way along time scales. The Morlet Wavelet is a plane wave modulated by a gaussian. The cross-wavelet power indicates the scales of higher covariance between two time series. This analysis gives the correlation between two time series as a function of the period of the signal and its time evolution with a 95% confidence level contour.

Figure 3a and 3b show each from top to bottom, the interplanetary magnetic field B_z-component measured by ACE, shifted by 35 minutes taking into account a solar wind velocity of 800 kms$\cdot$s^{-1}, the sunward B_x-component in the magnetotail observed by Cluster, and the cross-wavelet power spectrum between them. Figure 3a shows data from the second plasma sheet crossing and Figure 3b from the third (see Figure 1). We have used 16 second averages for the interplanetary and the magnetospheric field components. The Cluster B_x-component was filtered with a polynomial fit (3rd order)

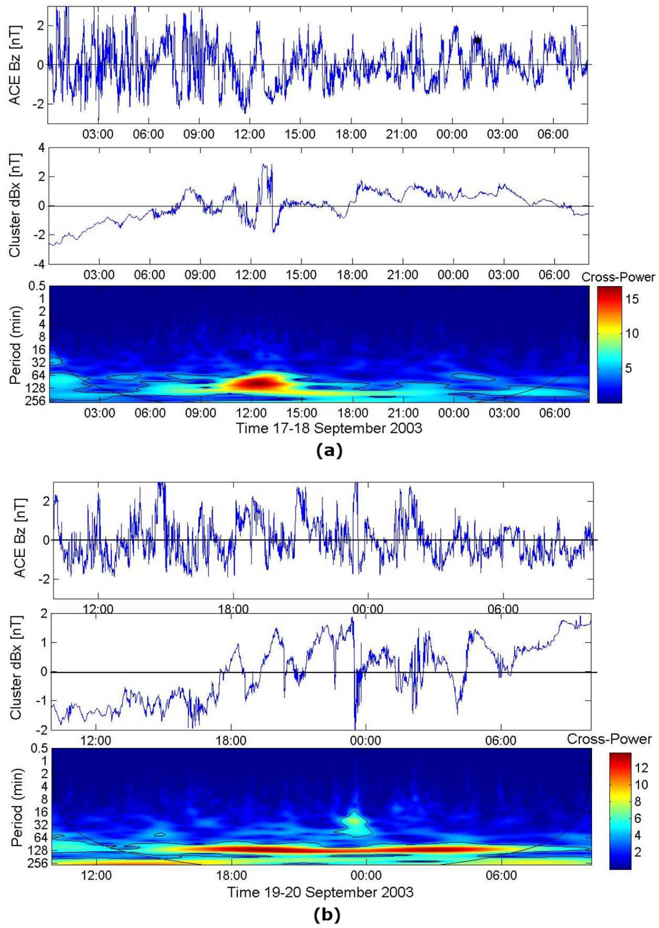

Fig. 3. Figure 3a: Cross-wavelet analysis of ACE interplanetary B_z component and of Cluster dB_x for September 17 (03:00 UT) to 18 (08:00 UT), 2003.Figure 3b: Same as Figure 3a, but for September 19 (10:00 UT) to September 20 (10:00 UT), 2003.

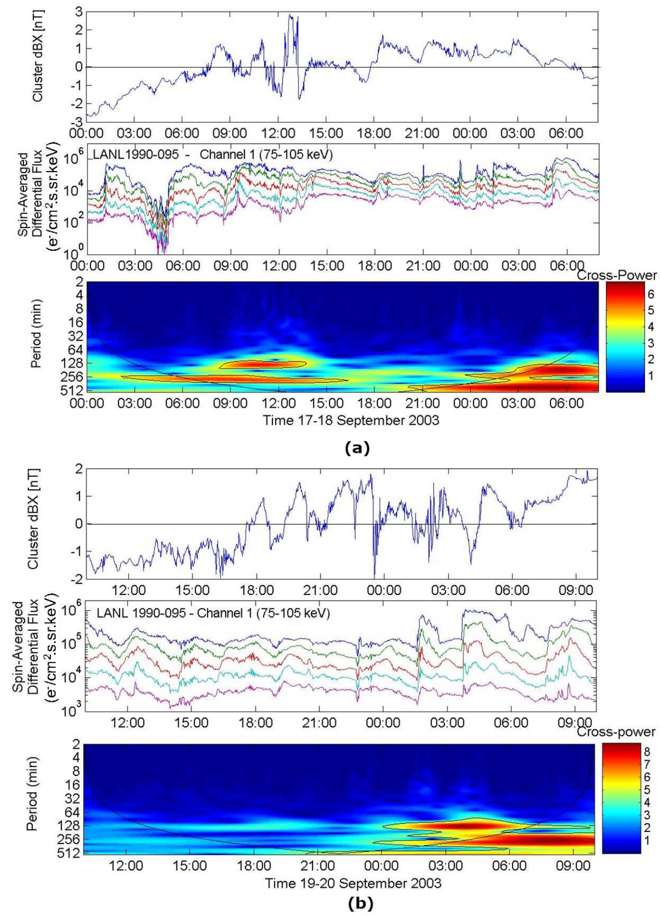

Fig. 4. Figure 4a: Cross-wavelet power between Cluster dB_x and the first (75 - 105 keV) of five electron channels from spacecraft LANL 1990-095, for September 17 (00:00 UT) to September 18 (08:00 UT), 2003. Figure 4b: Same as Figure 4a, but for September 19 (10:00 UT) to September 20 (10:00 UT), 2003.

to remove the longest variations. The cross-wavelet spectrum in the third panel covers the period range from 1 minute to $\sim$ 4 hours. We observe enhanced power around 2-3 hours for the second plasma sheet crossing on September 17/18, 2003, and enhanced power of about 2 hours during the third crossing on September 19/20, 2003 period. For the crossing on September 17/18 the power is more concentrated around 12:00 UT, because of the strong fluctuations in B_z and B_x. During the September 19/20 crossing, a strong cross-power is seen around 2 hours during most of the interval. In this event we can see the presence of quasi-periodical fluctuations in the Cluster B_x data, of the same time. In ACE we see strong fluctuations around this time, but with presence of high frequency oscillations.

As seen from Figure 2 the fluctuations in the B_x-component are proportional to the pressure change which is again a measure of the amount of substorms. In comparing the B_x-component with substorms closer to Earth at geosynchronous orbit the cross-power was calculated between the Cluster B_x-component and the electron flux at geosynchronous orbit. Figure 4a and b show the cross-wavelet power of the Cluster dB_x and the LANL 1990-095 spacecraft electron flux data. Channels 0 to 4 ($\sim$ 50 to 315 keV) are shown. The cross-wavelet power was calculated between Cluster dB_x and channel 1 (75-105 keV). For September 17/18 a significant cross-power is observed around 2 hours during a short time ($\sim$ 09:00-13:00 UT) and an extended cross-power around 3-4 hours for most of the interval. Figure 4b shows for September 19/20 a cross-power at 2 hours which is significantly enhanced after $\sim$ 00:00 UT of September 20.

4. Conclusions

We have shown here that the September 2003 fast solar wind streams and their embedded large amplitude Alfvén waves have a direct influence on the recurrent substorm activity observed. In linking the recurrent 2-4 hour substorm activity directly to the periodicities in the solar wind Alfvén waves we not only confirm the results of Borovsky et al. [4], but show that the causative driver in the solar wind are prolonged periods of intermittently large negative IMF B_z that can lead to heating of the plasma sheet and to substorm activity.

We have demonstrated the direct link between the interplanetary magnetic field (IMF) B_z and the sunward magnetic B_x-component measured with Cluster in the plasma sheet, and the subsequent injection signatures seen at geosynchronous orbit.

In the wavelet spectrum enhanced power is observed between 2-4 hours which means that a loading/unloading process takes place every 2-4 hours. B_x is the largest magnetic field component in the plasma sheet (B_y and B_z are about zero) and therefore it is proportional to the pressure. The change in pressure is related to substorms. In comparing this period with substorms at geosychronous orbit, the wavelet spectra show enhanced power also in the 2-4 hour period. The triggering of this kind of substorms seems to be pressure driven and direct, in contrast to the sawtooth events described by Henderson et al. [7] where the magnetosphere is under SMC-like conditions where triggering may be controlled more by internal stability thresholds than distinct external triggers.

Further work remains to be done to establish the timing (phase) relationship between the correlations (Solar wind to plasma sheet, plasma sheet to geosynchronous), which we did not attempt here.

Acknowledgements

The authors would like to thank the ACE SWEPAM and MAG teams for making solar wind plasma and magnetic field data available. We thank the Kyoto World Data Center for Geomagnetism for the Dst and AE indices. E. Echer and F. L. Guarnieri thank FAPESP for their post-doctoral fellowships (04/11115-4 and 04/14784-4) and their financial supports (05/03501-4).

References

1. Balogh, A., Carr, C. M., Acuna, M. H., Dunlop, M. W., Beek, T. J., Brown, P., Fornacon, K. H., Georgescu, E., Glassmeier, K.-H., Harris, J., Musmann, G., Oddy, T., and Schwingenschuh, K., The Cluster Magnetic Field Investigation: overview of in-flight performance and initial results, *Ann. Geophys., 19*, 1207–1217, 2001.
2. Belcher, J. W. and Davis Jr., L., Large Amplitude Alfvèn waves in the interplanetary medium, 2, *J. Geophys. Res., 76*, 3534, 1971.
3. Blanchard, G. T., Lyons, L. R., and Spann, J., Predictions of substorms following northward turnings of the interplanetary magnetic field, *J. Geophys. Res.,105*, 375–84, 2000
4. Borovsky, J. E., Nemzek, R. J., and Belian, R. D., The occurrence rate of magnetospheric substorm onsets: Random and period substorms, *J. Geophys. Res., 98*, 3897, 1993.
5. Escoubet, C. P., Fehringer, M., and Goldstein, M., The Cluster mission, *Ann. Geophys., 19*, 1197–1200, 2001.
6. Harvey, K., Suess, S., Aschwanden, M., Guhathakurta, M., Harvey, J., Hathaway, D., LaBonte, B., Sheeley, N., and Tsurutani, B. T., A NASA workshop on coronal holes near solar maximum and over the solar cycle, Washington: NASA, 2000.
7. Henderson M. G., Reeves, G. D., Skoug, R., Thomsen, M. T., Denton, M. H., Mende, S. B., Immel, T. J., Brandt, P. C., and Singer, H. J., Magnetospheric and auroral activity during the 18 April 2002 sawtooth event, *J. Geophys. Res., 111*, A01S90, doi:10.1029/2005JA011111, 2005.
8. Hollweg, J. V., Some physical processes in the solar wind, *Rev. Geophys. Space Phys., 16*, 689, 1978.
9. Lee, D. Y., Lyons, L. R., and Yumoto, K., Sawtooth oscillations directly driven by solar wind dynamic pressure enhancements, *J. Geophys. Res., 109*, A04202, 2004.
10. Lyons, L. R., Blanchard, G. T., Samson, J. C., Lepping, R. P., Yamamoto, T., and Moretto, T., Coordinated observations demonstrating external substorm triggering, *J. Geophys. Res., 102*, 27039-51, 1997.
11. Lyons, L. R., Lee, D.-Y., Thorne, R. M., Horne, R. B., and Smith, A. J., Solar wind-magnetosphere coupling leading to relativistic electron energization during high-speed streams, *J. Geophys. Res., 110, A11202*, doi: 10.1029/2005JA011254, 2005.
12. Percival, D. B. and Walden, A. T., Wavelet Methods for Time Series Analysis, Cambridge University Press, 2000.
13. Rème, H., et al., First multispacecraft ion measurements in and near the Earth's magnetosphere with the identical Cluster Ion Spectrometry (CIS) experiment, *Ann. Geophys., 19*, 1303–1354, 2001.
14. Reeves, G. D., Belian, R. D., Cayton, T. C., Henderson, M. G., Christensen, R. A., McLachlan, P. S., and Ingraham, J. C., Using Los Alamos geosynchronous energetic particle data in support of other missions. In Satellite-Ground Based Coordination Source Book, edited by M.N. Wild M. Lockwood, and H.J. Opgenoorth, pages 263–272. ESA Publications, ESTEC, Noordwijk, The Netherlands, June 1997.
15. Sheeley, N. R., Harvey Jr., J. W., and Feldman, W. C., Coronal holes, solar wind streams, and recurrent geomagnetic disturbances, 1973–1976, *Solar Physics, 49*, 271, 1976.
16. Sheeley, N. R., Harvey Jr., J. W., and Feldman, W. C., Coronal holes, solar wind streams, and geomagnetic activities during new sunspot cycle, *Solar physics, 59*, 159, 1978.
17. Sheeley, N. R. and Harvey Jr., J. W., Coronal holes, solar wind streams, and geomagnetic disturbances during 1978 and 1979, *Solar Physics, 70*, 237, 1981.
18. Smith, E. J. and Wolf, J. H., Observations of interaction regions and corotating shocks between one and five AU: Pioneers 10 and 11, *Geophys. Res. Lett., 3*, 137, 1976.
19. Stone, E. C., Frandsen, A. M., Mewaldt, R. A., Christian, E. R., Margolies, D., Ormes, J. F., and Snow, F., The advance composition explorer, *Space Science Rev., 86*, 1–22, 1998.
20. Torrence, C. and Compto, G. P., A Practical Guide to Wavelet Analysis, *Bulletin of the American Meteorological Society, 79*, 61–78, 1998.
21. Tsurutani, B. T., Gonzalez, W. D., Gonzalez, A. L. C., Tang, F., Arballo, J. K., and Okada, M., Interplanetary origin of geomagnetic activity in the declining phase of the solar cycle, *Geophys. Res., 100*, 21717–21733, 1995.
22. Wilken, B., et al., First results from the RAPID imaging energetic particle spectrometer on board Cluster, *Ann. Geophys., 19*, 1355–1366, 2001.